Identification of *Azadinium poporum* (Dinophyceae) in the Southeast Pacific: morphology, molecular phylogeny, and azaspiracid profile characterization

URBAN TILLMANN[1]*, NICOLE TREFAULT[2], BERND KROCK[1], GÉNESIS PARADA-POZO[2], RODRIGO DE LA IGLESIA[3] AND MÓNICA VÁSQUEZ[3]

[1]ALFRED WEGENER INSTITUTE, HELMHOLTZ CENTRE FOR POLAR AND MARINE RESEARCH, AM HANDELSHAFEN 12, D-27570 BREMERHAVEN, GERMANY, [2]CENTER FOR GENOMICS AND BIOINFORMATICS, FACULTY OF SCIENCES, UNIVERSIDAD MAYOR, CAMINO LA PIRÁMIDE 5750, HUECHURABA, SANTIAGO, CHILE AND [3]DEPARTMENT OF MOLECULAR GENETICS AND MICROBIOLOGY, PONTIFICIA UNIVERSIDAD CATÓLICA DE CHILE, AV. LIBERTADOR BERNARDO O´HIGGINS 340, SANTIAGO, CHILE

*CORRESPONDING AUTHOR: urban.tillmann@awi.de

Azaspiracids (AZA), a group of lipophilic phycotoxins, are produced by some species of the marine dinophycean genus *Azadinium*. AZA have recently been detected in shellfish from the Southeast Pacific, however, AZA-producing species have not been recorded yet from the area. This study is the first record of the genus *Azadinium* and of the species *Azadinium poporum* from the Pacific side of South America. Three strains of *A. poporum* from Chañaral (Northern Chile) comply to the type description of *A. poporum* by the presence of multiple pyrenoids, in thecal plate details, and in the position of the ventral pore located on the left side of the pore plate. Molecular phylogeny, based on internal transcribed spacer and large subunit ribosomal DNA sequences, revealed that Chilean strains fall in the same ribotype clade as European and strains from New Zealand. Analyses of AZA profiles using LC–MS/MS showed an identical profile for all three strains with the presence of AZA-11 and two phosphorylated AZA. This is the first confirmation of the presence of AZA producing *Azadinium* in the Chilean coastal area and underlines the risk of AZA shellfish and concomitant human contamination episodes in the Southeast Pacific region.

KEYWORDS: *Azadinium*; azaspiracids; Southeast Pacific; Chile

INTRODUCTION

The Humboldt Current flowing along the west coast of South America is one of the major ocean current systems of the world where cold, nutrient-rich upwelling water drives high rates of primary and secondary productivity. Consequently, the water masses off Chile are among the most productive marine areas on a global scale (Alheit and Bernal, 1993; Daneri *et al.*, 2000) and marine fisheries are a key component of the Chilean economy (Gelcich *et al.*, 2010). During strong upwelling periods, occurring typically in winter and spring, diatoms dominate the system. However, dinophytes and other smaller sized flagellates may dominate during weakened upwelling periods (typically in summer and autumn) and El Niño periods when nutrient availability is reduced (Iriarte and González, 2004; Ochoa *et al.*, 2010). This is of particular importance as many members of the Dinophyceae or other planktonic flagellates are known for the production of potent toxins and other bioactive compounds. This phytoplanktonic class may form Harmful Algal Blooms (HAB) causing human health problems, massive killing of fish, birds or mammals and/or other ecosystem disruptions (Smayda, 1997; Hallegraeff, 2003, 2014).

Records of phycotoxins and potentially toxic plankton species as well as reports of HAB for the Humboldt Current system off Chile indicate the presence of almost all known phycotoxins. Pectenotoxins and okadaic acid including dinophysistoxins in plankton, filter feeders, and in cells of local *Dinophysis* spp. are common (Blanco *et al.*, 2007; Krock *et al.*, 2009a; Trefault *et al.*, 2011). Moreover, yessotoxins are reported both in shellfish (Yasumoto and Takizawa, 1997) and in plankton samples (Krock *et al.*, 2009a), and blooms of the producing species *Lingulodinium polyedra* have been also recorded (Álvarez *et al.*, 2011). Spirolides are found in shellfish in northern Chile (Álvarez *et al.*, 2010), and gymnodimines were recently detected in Chile for the first time (Trefault *et al.*, 2011). In Northern Chile off Bahía Inglesa, blooms of *Pseudo-nitzschia australis* and detection of domoic acid above regulatory levels in scallops have been reported (Suárez-Isla *et al.*, 2002). Paralytic shellfish poisoning (PSP) is a major problem in southern Chile (Lagos, 1998; Guzmán *et al.*, 2002). Nevertheless it is present in the Humboldt Current system, and blooms of *Alexandrium* as well as PSP toxins in shellfish were detected in several aquaculture sites in northern Chile (Álvarez *et al.*, 2009).

The group of azaspiracids (AZA) were recently also found in the area (Álvarez *et al.*, 2010; López-Rivera *et al.*, 2010; Trefault *et al.*, 2011). AZA are the most recently identified group of lipophilic marine biotoxins, which are associated with human incidents of shellfish poisoning (Twiner *et al.*, 2014). This group of compounds has been reported in shellfish from numerous geographical sites, such as the Atlantic coasts of various European countries including Denmark, France, Ireland, Norway, Portugal, Spain, Sweden and the United Kingdom (James *et al.*, 2002; Braña Magdalena *et al.*, 2003; Amzil *et al.*, 2008; Vale *et al.*, 2008). AZA are known from the Pacific coast of the United States (Trainer *et al.*, 2013) and Mexico (García-Mendoza *et al.*, 2014), from the Atlantic coasts of NW Africa (Taleb *et al.*, 2006) and Canada (M. Quilliam, personal communication in Twiner *et al.*, 2008), and from the Asian Pacific off China (Yao *et al.*, 2010) and Japan (Ueoka *et al.*, 2009). With respect to South America, AZA have been found on both the Atlantic and Pacific coasts in Brazil (Massucatto *et al.*, 2014), Argentina (Turner and Goya, 2015) and Chile (Álvarez *et al.*, 2010; López-Rivera *et al.*, 2010), respectively.

AZA are produced by some species of the family Amphidomataceae. This was discovered in 2009 driven by the targeted search for the planktonic source of AZA (Krock *et al.*, 2009b) with the first described species *Azadinium spinosum* Elbrächter et Tillmann (Tillmann *et al.*, 2009). Among the eleven species of the genus *Azadinium* (Tillmann and Akselman, 2016), three have been found to produce AZA (i.e. *Azadinium spinosum*, *Azadinium poporum* Tillmann et Elbrächter, *Azadinium dexteroporum* Percopo et Zingone) (Krock *et al.*, 2012; Percopo *et al.*, 2013). AZA have also been found in the related species *Amphidoma languida* Tillmann, Salas et Elbrächter (Tillmann *et al.*, 2012).

Just as for records of AZA in shellfish there is increasing evidence that species of *Azadinium* and *Amphidoma* have a wide geographical distribution in both coastal and open ocean areas of both the North and South Atlantic and Pacific (Tillmann *et al.*, 2014b). For the Atlantic side of South America, *Azadinium* now is retrospectively known to have been present almost two decades ago and at least three bloom episodes of a diverse community of *Azadinium* species occurred in 1990, 1991 and 1998 (Akselman and Negri, 2012; Akselman *et al.*, 2014; Tillmann and Akselman, 2016). In addition, the presence of an AZA producing *Azadinium*, an AZA-2 producing *A. poporum* in the Argentinean coastal area, was recently confirmed (Tillmann *et al.* 2016). *A. poporum* producing the same AZA compound, but differing significantly in ribosomal sequence data from the Argentinean population, was recorded in the Gulf of Mexico (Luo *et al.*, 2016). In the Pacific Ocean, *Azadinium* has been recorded in Korea, China and New Zealand (Potvin *et al.*, 2012; Gu *et al.*, 2013; Smith *et al.*, 2016). However, on the Pacific side of South America there has been only

one record of a species determined as *A. spinosum* on the Pacific coast of Mexico (Hernández-Becerril *et al.*, 2012). Despite the known presence of AZA in Chile (Álvarez *et al.*, 2010; López-Rivera *et al.*, 2010), the causative species in Chilean coastal waters thus have not been detected or identified yet. This is important because it is quite likely that the diversity of the Amphidomataceae is not yet fully explored and thus new toxigenic species might be present. Knowledge on the species present is an indispensable prerequisite for any monitoring and/or early warning system to be successfully implemented. This is especially true for small and inconspicuous species like *Azadinium* whose routine detection and identification require molecular detection tools, which are only available for known species. Large areas of the Chilean coast are difficult to access for routine plankton sampling and thus detailed knowledge on the species composition of the small plankton fraction is rare. The aim of the present study was thus to specifically search for the presence

of *Azadinium* and to obtain and grow isolates of *Azadinium* from Chile for a thorough morphological, molecular and toxinological characterisation.

METHOD

Field campaign

In 2014, a sampling campaign was setup to study effects of heavy metal contamination on plankton in the Chañaral area, a site heavily affected by copper deposition from the local mining industry. As a side aspect of this campaign, plankton samples were taken for determining microalgal toxins and for detecting and characterising potentially toxic species with the special aim for AZA and *Azadinium*.

Sampling

Seawater samples were taken from the Chañaral area at three stations (Fig. 1) aboard a fishing boat from March 11th to March 12th, 2014. Details of sampling stations are shown in Table I. At each station, three 5 L Niskin bottle samples (5 m depth) and three vertical plankton net tows ($\geq$23 μm, 20 m depth) were collected and combined to yield one large volume water sample and one plankton net concentrate. Water samples were pre-filtered on-board using a 150 μm nylon net, to exclude large particles and zooplankton, and stored in the dark in acid-washed carboys. Physicochemical parameters of seawater were registered *in situ* using a CTD-O (SBE19). For a qualitative and quantitative characterization of the plankton community, half a liter of Niskin bottle samples from each station was gently concentrated by gravity filtration using a 3-μm polycarbonate filter. The plankton concentrate was washed from the filter and fixed with Lugol's iodine (1% final concentration). For cell abundance estimations using flow cytometry, subsamples of 1.35 mL were taken
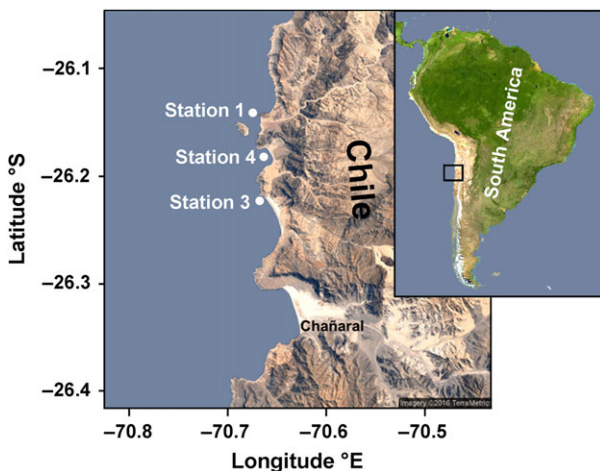

Fig. 1. Study area and sampling stations in the Chañaral area, off northern Chile, Southeast Pacific.

Table I: Chañaral area sampling data

Station	1	3	4
Sampling date	11.03.2014	12.03.2014	12.03.2014
Site	Pan de Azúcar	Playa La Lancha	Playa Blanca
Location (Lat; Long)	26°08′26.0″S; 70°41′15.2″W	26°13′27.4″S; 70°40′02.0″W	26°10′58.2″S; 70°39′45.7″W
Temperature (°C)	15.8	12.3	12.2
Salinity	34.5	34.6	34.6
O_2 (mL L^{-1})	5.61	6.03	6.05
Chlorophyll-*a* (mg m^{-3})	13.21	3.17	2.35
NO_3 (μmol L^{-1})	10.48	10.35	14.79
NO_2 (μmol L^{-1})	0.93	0.86	0.62
PO_4 (μmol L^{-1})	1.99	2.00	2.03
Si (μmol L^{-1})	9.56	9.37	7.94
PTX-2 (ng NT^{-1})	5	30	61
PTX-2sa (ng NT^{-1})	16	91	779

Si = silicate; PTX-2 = Pectenotoxin-2; PTX-2sa = Pectenotoxin-2-seco-acid; NT = net tow.

in triplicate, fixed with 150 μL of fixative solution (10% formaldehyde, 0.5% glutaraldehyde, 100 mM sodium borate pH 8.5), incubated for 20 min at room temperature and transferred to a nitrogen dry shipper (CXR500, Taylor Wharton) until transport to the laboratory, where they were maintained at −80 °C until analysis. For molecular detection of *Azadinium*, app. 5 L sample was filtered using a 47 mm diameter Swinnex holder system in a Masterflex 6-600 rpm peristaltic pump (Cole Parmer), and the biomass was collected onto 0.22 μm pore size filters (GSWP04700, Millipore). Filters were stored in 2 mL sterile cryovials and immediately deep frozen until transport to the laboratory and there, stored at −80 °C until analysis.

For AZA analysis, 1-L subsamples of the Niskin bottles were pre-screened through a 20 μm mesh-size Nitex sieve. Each sample was then filtered under gentle vacuum through 3 μm pore-size polycarbonate filters (Millipore). Filters were attached with the back to the inner wall of 50 mL centrifugation tubes and stored at −20 °C until analysis. For the analysis of other lipophilic toxins, plankton cell concentrates from net tows were added to a volume of 10 mL of seawater from the same sampling site and centrifuged at 4000 × *g* for 10 min at 4 °C. Pellets were stored at −20 °C until extracted in the laboratory.

Optical analysis of phytoplankton samples

Light microscopy Defined subsamples were settled in 1 mL sedimentation chambers. Depending on the cell size and/or abundance of different groups of microalgae, either the plankton content of the whole chamber or representative sub-areas were counted with an inverted microscope (Axiovert 40C, Zeiss, Göttingen, Germany).

Flow cytometry Cell abundances of heterotrophic bacteria (Het Bact), pico-cyanobacteria, i.e. *Synechococcus* (Syn), pico-eukaryotes (Pico-euk) and nano-eukaryotes (Nano-euk) were determined using a FACSCalibur BD flow cytometer equipped with an ion–argon laser delivering 15 mW at 488 nm (Becton Dickinson). Light scatter and fluorescence were normalized by adding 1 and 3-μm fluorescent beads to the samples. The data generated were processed using the CytoWin software.

Molecular identification of Azadinium in field samples

DNA was extracted from the biomass collected on the 0.22 μm pore size filters using a phenol:chloroform protocol according to Fuhrman *et al.* (1988). DNA integrity was checked by 0.8% agarose gel electrophoresis and DNA was quantified using the Qubit 2.0 Fluorimeter (Life Technologies). *Azadinium* cells were identified by amplification of the 28 S rRNA gene using primer pairs Apop62F (5′-GAT GCT CAA GGT GCC TAG AAA GTC-3′) and Apop148R (5′-CCT GCG TGT CTG GTT GCA-3′), specific for *A. poporum*, Asp48F (5′-TCG TCT TTG TGT CAG GGA GAT G-3′) and Asp120R (5′-GGA AAC TCC TGA AGG GCT TGT-3′) specific for *A. spinosum*, and Aob134F (5′-AGG GAT CGA TAC ACA AAT GAG TAC TG-3′) and Aob208R (5′-AAA CTC CAG GGACAT GGT AGT CTT A -3′), specific for *A. obesum* (Toebe *et al.*, 2013).

Amplifications were carried out using 20 μL PCR reaction containing 6.45 μL milliQ water, 4 μL of 5× Colorless GoTaq Flexi Buffer (Promega), 1.6 μL of 25 mM $MgCl_2$ (Promega), 0.4 μL of each primer (10 μM), 0.4 μL of dNTP (10 mM), 5 μL of 2 μg μL^{-1} BSA, 0.25 μL of 5 U μL^{-1} GoTaq Flexi DNA Polymerase (Promega) and 5 ng μL^{-1} of DNA. PCRs were performed in a Mastercycler Personal thermocycler (Eppendorf), with cycle conditions as follows: 5 min at 95 °C, followed by 33 cycles of 45 s at 95 °C, 30 s at 58 °C, 30 s at 72 °C and a final extension of 10 min at 72 °C.

Chemical analysis of field samples

Azaspiracids Filters attached to the back to the inner wall of 50-mL centrifugation tubes were manually rinsed with 1.5 mL methanol several times, until complete discoloration of the filters. The methanol extracts were transferred to high performance liquid chromatography (HPLC) vials and dried completely under a gentle nitrogen stream. Dried samples were taken up in 500 μL acetone and stored at −20 °C until analysis. AZA analysis was performed as described below.

Other lipophilic toxins Algal pellets were homogenized by ultrasonication (sonotrode HD 2070, Bandelin, Berlin, Germany; 1 min, cycle time 50%, 10% power) with 700 μL methanol. After homogenization, samples were centrifuged (Eppendorf 5415 R, Hamburg, Germany) at 16 100 × *g* at 4 °C for 15 min. Supernatants were transferred to spin-filters (pore-size 0.45 mm, Millipore Ultrafree, Eschborn, Germany) and centrifuged for 30 s at 800 × *g*. The filtrates were transferred to HPLC vials and stored at −20 °C until measurement.

Single reaction monitoring measurements Concentrations of lipophilic toxins were determined as described in Krock *et al.* (2008). Toxins analyzed included domoic acid (DA), gymnodimine (GYM), spirolides (SPX), dinophysistoxins (DTX) including okadaic acid (OA), pectenotoxins (PTX), yessotoxin (YTX) and AZA.

Azadinium poporum cultures

Cell isolation, culture growth, sampling for toxins and DNA Cells were isolated from a water sample taken at Station 1. A Niskin bottle sample (5 m depth) was pre-screened

(20 μm Nitex gauze), gently concentrated by gravity filtration using a 3-μm polycarbonate filter, and examined using a stereomicroscope (Olympus SZH-ILLD; Olympus, Hamburg, Germany) with dark field illumination. From these preparations, clonal cultures of "*Azadinium*-like cells", defined by general size, shape and their characteristic swimming pattern, were established by isolation of single cells by micro-capillary into single wells of 96-well plates each prefilled with 0.3 mL of a natural seawater medium prepared with sterile-filtered (0.2 μm VacuCap filters, Pall Life Sciences, Dreieich, Germany) Antarctic seawater (salinity: 34 psu, pH adjusted to 8.0) and enriched with 1/10 strength K-medium (Keller *et al.* 1987; slightly modified by omitting addition of ammonium ions). In this manner, three clonal isolates were established and designated as strain 1-C11, 1-D5 and 2-B9.

For qualitative toxin analysis, strains were grown in 250 mL plastic culture flasks at 15 °C under a photon flux density of 60 μmol m^{-2} s^{-1} on a 16:8 h light:dark photocycle. For each harvest, cell density was determined by settling Lugol-fixed samples and counting >800 cells under an inverted microscope. Densely grown strains (ranging from about 10 to 100 × 10^4 cells mL^{-1}) were harvested in four 50 mL centrifugation tubes. After centrifugation (Eppendorf 5810 R, Hamburg, Germany) at 3220 × *g* for 10 min, the four pellets were combined in a microtube, centrifuged again (Eppendorf 5415, 16 000 × *g*, 5 min), and stored at −20 °C until use. Growth and harvest procedures were repeated several times (total volume harvested ranging from 1.8 to 2.0 L for different isolates) to yield a total number of at least 3.8 × 10^7 cells per isolate. Toxin cell quota of each strain was estimated as the mean of four quantitative analyses of independent cultures grown under the culture conditions as outlined above. For each analysis, cell density of the respective culture was estimated and 50 mL culture volume was concentrated as described above.

For DNA extraction, each strain was grown in 65 mL plastic culture flasks under the standard culture conditions described above. 50 mL of healthy and growing culture (based on stereomicroscopic inspection of the live culture) were harvested by centrifugation (Eppendorf 5810 R, Hamburg, Germany; 3220 × *g* for 10 min). Each pellet was transferred to a microtube, again centrifuged (Eppendorf 5415, 16 000 × *g*, 5 min), and stored frozen at −80 °C until DNA extraction.

Microscopy

Observation of living or fixed (formalin: 1% final concentration; or neutral Lugol-fixed: 1% final concentration) cells was carried out using an inverted microscope (Axiovert 200M, Zeiss, Germany) and a compound microscope (Axiovert 2, Zeiss, Germany), both equipped with differential interference contrast optics. Photographs were taken with a digital camera (Axiocam MRc5, Zeiss, Germany).

Cell length and width were measured at 1000× microscopic magnification using Zeiss Axiovision software (Zeiss, Germany) and freshly fixed cells (formalin, final concentration 1%) from dense but healthy and growing cultures (based on stereomicroscopic inspection of the live culture) at late exponential phase. For scanning electron microscopy (SEM), cells were collected by centrifugation (Eppendorf 5810 R, Hamburg, Germany, 3220 × *g* for 10 min.) of 15 mL culture. The supernatant was removed and the cell pellet re-suspended in 60% ethanol in a 2 mL microtube for 1 h at 4 °C to strip off the outer cell membrane. Subsequently, cells were pelleted by centrifugation (5 min, 16 000 × *g*, Eppendorf centrifuge 5415 R) and re-suspended in a 60:40 mixture of deionized water and seawater for 30 min at 4 °C. After centrifugation and removal of the diluted seawater supernatant, cells were fixed with formalin (2% final concentration in a 60:40 mixture of deionized water and seawater) and stored at 4 °C for 3 h. Cells were then collected on polycarbonate filters (Millipore, 25 mm Ø, 3 mm pore-size) in a filter funnel where all subsequent washing and dehydration steps were carried out. A total of eight washings (2 mL MilliQ-deionized water each) were followed by a dehydration series in ethanol (30, 50, 70, 80, 95, 100%; 10 min each). Filters were dehydrated with hexamethyldisilazane (HMDS), first in 1:1 HMDS:EtOH followed by two times 100% HMDS, and then stored under gentle vacuum in a desiccator. Finally, filters were mounted on stubs, sputtercoated (Emscope SC500, Ashford, UK) with gold-palladium and viewed under a scanning electron microscope (FEI Quanta FEG 200, Eindhoven, Netherlands). Some SEM micrographs were presented on a black background using Adobe Photoshop 6.0 (Adobe Systems, San Jose, USA).

Molecular phylogeny

DNA extraction, PCR amplification and sequencing DNA was extracted from the cell pellets (see above) using DNeasy extraction kit (Qiagen) following the protocol provided by the manufacturer, with few modifications. Lysis was made using warm lysis buffer (65 °C), cells were transferred to a glass beads solution and fast prep to disrupt them (2 × 20 s at 6500 rpm), 4 μL of RNAse was added, and elution was made in 50 μL of elution buffer.

PCR for internal transcribed spacer ribosomal DNA (ITS rDNA) was performed using primers ITSa (5′-CCAAGCTTCTAGATCGTAACAAGG(ACT)TCCGTAGGT-3′) and ITSb (5′-CCTGCAGTCGACA(GT)ATGCTTAA(AG)TTCAGC(AG)GG-3′) (Adachi *et al.,*

1996). PCR for the large subunit ribosomal DNA (LSU rDNA) was performed using primers D1C (5′-ACCCG CTGAATTTAAGCATA-3′) and D2R (5′-CCTTGG TCCGTGTTTCAAGA-3′) (Scholin *et al.*, 1994). Genomic DNA was amplified in 20 μL PCR reaction containing 16.3 μL milliQ water, 2.0 μL of 10× HotMaster Taq Buffer (Eppendorf, which included MgCl$_2$), 0.2 μL of each primer (10 μM), 0.2 μL of dNTP (10 μM), 0.1 HotMaster Taq polymerase (Eppendorf) and 10 ng μL^{-1} of DNA. PCRs were performed in a Mastercycler Personal termocycler (Eppendorf), with PCR reaction conditions for ITS amplification: 4 min at 94 °C, followed by 10 cycles of 50 s at 94 °C, 40 s at 58 °C, 1 min at 70 °C, and then 30 cycles of 45 s at 94 °C, 45 s at 50 °C, 1 min at 70 °C, and a final extension of 5 min at 70 °C, and for LSU amplification as follows: 2 min at 94 °C, followed by 30 cycles of 30 s at 94 °C, 30 s at 55 °C, 2 min at 65 °C, and a final extension of 10 min at 65 °C.

PCR products were purified with MinElute PCR purification kit (Qiagen) and sequenced using an ABI 3130 XL capillary sequencer (Applied Biosystems). For this, sequencing reaction contained 1 μL of purified PCR product, 1.5 μL Big Dye Buffer (Life Technologies), 0.3 μL Big Dye, 1 μL of PCR primer (forward or reverse) and 7.2 μL of milliQ water. Conditions for sequencing reaction were as follows: 1 min at 96 °C, followed by 25 cycles of 10 s at 96 °C, 5 s at 50 °C and 4 min at 60 °C. Sequencing products were purified with Agencourt CleanSEQ—Dye Terminator Removal (Beckman Coulter) and sequenced in both directions.

Sequences were examined and checked for accuracy of base-calling using the ABI Sequencing Analysis software. Sequences were assembled using the AlignX module from Vector NTI software (Life Technologies).

Phylogenetic analysis   ITS and LSU rDNA sequences from *A. poporum* and *Azadinium dalianense* were gathered from GenBank (release 211). These sequences were combined with the ITS and LSU rDNA sequences obtained from the new *A. poporum* strains from Chile, resulting a total of 43 ITS rDNA sequences and 31 LSU rDNA sequences. Details of *A. poporum* strains used in this study are listed in Suppl. Table S01.

Phylogenetic analyses were performed using maximum likelihood (ML) and Bayesian inference methods, using MEGA 6 (Tamura *et al.*, 2013) and MrBayes v3.2.5 (Huelsenbeck and Ronquist, 2001), respectively. For this, ITS and LSU sequences were separately aligned using Muscle (Edgar, 2004) with 32 iterations and manually inspected. Alignment files (*.mas, *.nexus) are available upon request. For ML, aligned sequences were subjected to module Model Selection from MEGA 6 to find the best nucleotide substitution model, and to phylogenetic

reconstruction with K2 + G model for nucleotide substitutions (Kimura, 1980) with five discrete Gamma categories and 1000 bootstrap replications, both for ITS and LSU sequences. Then 620 and 617 sites were included in the analysis of ITS rDNA and LSU rDNA, respectively, with a complete deletion of gaps and Nearest-Neighbor-Interchange (NNI) as ML heuristic method. For Bayesian analysis, the best nucleotide substitution model was found using MrModeltest (https://github.com/nylander/ MrModeltest2), with a hierarchical Likelihood Ratio Test (hLRT) and Bayesian inference was performed with F81 I + G (Felsenstein, 1981) for ITS and with SYM I + G (Zharkikh, 1994) for LSU, and 10 000 replications in each case. Statistical support values (ML-BS: ML-bootstrap support and B-PP: Bayesian posterior probability) were included on the resulting best scoring ML-tree.

Genetic pairwise similarities between both ITS and LSU sequences from *A. poporum* were calculated after global alignments using ClustalW using the AlignX module from Vector NTI software (Life Technologies).

Sequences were deposited in NCBI under accession numbers KX133010–KX133015.

Chemical analysis of AZA

Single reaction monitoring measurements   Water was deionized and purified (Milli-Q, Millipore, Eschborn, Germany) to 18 M cm^{-1} or better quality. Formic acid (90%, p.a.), acetic acid (p.a.) and ammonium formate (p.a.) were purchased from Merck (Darmstadt, Germany). The solvents, methanol and acetonitrile, were HPLC grade (Merck, Darmstadt, Germany).

Mass spectral experiments were performed to survey for a wide array of AZA with an analytical system consisting of an AB-SCIEX-4000 Q Trap, triple quadrupole mass spectrometer equipped with a TurboSpray interface coupled to an Agilent model 1100 LC. The LC equipment included a solvent reservoir, in-line degasser (G1379A), binary pump (G1311A), refrigerated autosampler (G1329A/G1330B), and temperature-controlled column oven (G1316A).

Cell pellets were extracted with 500 μL acetone by ultrasonication (Sonotrode, Bandelin HP2070, Berlin, Germany; 70 s; 70 cycles; 10% power). After homogenization, extracts were centrifuged (Eppendorf 5415 R) at 16 100 × *g* at 4 °C for 10 min. Each supernatant was transferred to a 0.45 μm pore-size spin-filter (Ultrafree, Millipore, Eschborn, Germany) and for LC–MS/MS analysis.

Separation of AZA (5 μL sample injection volume) was performed by reverse-phase chromatography on a C8 phase. The analytical column (50 × 2 mm) was packed with 3 μm Hypersil BDS 120 Å (Phenomenex,

Aschaffenburg, Germany) and maintained at 20 °C. The flow rate was 0.2 mL min^{-1}, and gradient elution was performed with two eluents, where eluent A was water and B was acetonitrile/water (95:5 v/v), both containing 2.0 mM ammonium formate and 50 mM formic acid. Initial conditions were 8 min column equilibration with 30% B, followed by a linear gradient to 100% B in 8 min and isocratic elution until 18 min with 100% B then returning to initial conditions until 21 min (total run time: 29 min).

AZA profiles were determined in one period (0–18) min with curtain gas: 10 psi, CAD: medium, ion spray voltage: 5500 V, temperature: ambient, nebulizer gas: 10 psi, auxiliary gas: off, interface heater: on, declustering potential: 100 V, entrance potential: 10 V, exit potential: 30 V. Single reaction monitoring (SRM) experiments were carried out in positive ion mode by selecting the transitions shown in Table II. In field samples, AZA were measured against an external standard solution of AZA-1 [certified reference material (CRM) programme of the IMB-NRC, Halifax, Canada]. *Azadinium poporum* cultures were calibrated against an external standard solution of AZA-1 (CRM) and expressed as AZA-1 equivalents.

Precursor ion experiments Precursors of the fragments m/z 348 and m/z 362 were scanned in the positive ion mode from m/z 400 to 950 under the following conditions: curtain gas: 10 psi, CAD: medium, ion spray voltage: 5500 V, temperature: ambient, nebulizer gas: 10 psi, auxiliary gas: off, interface heater: on, declustering potential: 100 V, entrance potential: 10 V, collision energy: 70 V, exit potential: 12 V.

Product ion spectra Product ion spectra were recorded in the enhanced product ion mode in the mass range from m/z 150 to 930. Positive ionization and unit resolution mode were used. The following parameters were applied: curtain gas: 10 psi, CAD: medium, ion spray voltage: 5500 V, temperature: ambient, nebulizer gas: 10 psi, auxiliary gas: off, interface heater: on, declustering potential: 100 V, collision energy spread: 0, 10 V, collision energy: 70 V.

Spike experiment One cell pellet of strain 1-C11 was spiked with 30 μL of a 1 ng μL^{-1} AZA-1 solution and another pellet with 30 μL of a 1 ng μL^{-1} AZA-2 solution. 120 μL acetone was added to both samples for homogenization and extraction as described above.

RESULTS

Field data

Sampling site description, Hydrography and Chemistry
The geographic location of the three sampling stations inside the Chañaral area, in the Southeast Pacific, is

Table II: Mass transitions m/z (Q1 > Q3 mass) and their respective AZA

Mass transition	Toxin	Collision energy (CE) [V]
716 > 698	AZA-33	40
816 > 798	AZA-39	40
816 > 348	AZA-39	70
828 > 658	AZA-3	70
828 > 810	AZA-3	40
830 > 812	AZA-38	40
830 > 348	AZA-38	70
842 > 672	AZA-1	70
842 > 824	AZA-1, AZA-40	40
842 > 348	AZA-40	70
844 > 826	AZA-4, AZA-5	40
846 > 828	AZA-37	40
846 > 348	AZA-37	70
854 > 836	AZA-41	40
854 > 670	AZA-41	70
854 > 360	AZA-41	70
856 > 672	AZA-2	70
856 > 838	AZA-2	40
858 > 840	AZA-7, AZA-8, AZA-9, AZA-10, AZA-36	40
858 > 348	AZA-36	70
868 > 362	Undescribed	70
870 > 852	Me-AZA-2, AZA-42	40
870 > 360	AZA-42	
872 > 854	AZA-11, AZA-12	40
910 > 892	Undescribed	40
936 > 918	AZA-2 phosphate	40
952 > 818	AZA-11 phosphate	40

shown in Fig. 1. Physicochemical properties of the seawater at the depth of sampling at each of the stations show that temperature and the average chlorophyll *a* was higher in the stations near Pan de Azúcar Island (Station 1) compared to Playa La Lancha and Playa Blanca (Stations 3 and 4, Table I). A high fluorescence at Station 1, which was close to Pan de Azúcar creek, was evident. Temperature ranged between 12.2 and 15.8 °C with higher temperature at Station 1, the most inshore station. Salinity was around 34.5 and showed no major variation between the sampling sites. Nutrient levels were moderately high (NO_3 > 10 μM, PO_4 ≥ 2 μM, Silicate > 7 μM) and similar for all three sampling stations (Table I).

Plankton composition
Flow cytometry measurements indicated that Stations 1, 3 and 4 were similar in the general pattern of abundance of the different plankton groups (Table III). *Synechococcus* spp. showed the highest abundance followed by pico-eukaryotes and nano-eukaryotes. At Station 3 pico-eukaryotes with an estimated cell size between 1 and 2 μm were the most abundant (Table III). Nano-eukaryotes, which are in the cell size range of *Azadinium* species, were more abundant in

Table III: Abundance of the most important plankton species/groups (cells L^{-1} for the larger size fraction quantified with light microscopy and 10^3 cells mL^{-1} for the small size fraction analyzed with flow cytometry)

Species	Station		
	1	3	4
Light microscopy			
Dinophysis sp.	1116	648	792
Dinophysis caudata	36	24	24
Tripos muelleri	1236	768	1272
Tripos furca	196	144	384
Protoperidinium spp.	1208	1461	1224
Azadinium-like	6840	0	1584
Guinardia striata	168 460	49 128	46 296
Guinardia delicatula	10 900	7776	5304
Small naked dinophyceae	5000	360	1056
Large ciliates (>20 μm)	1620	72	360
Small ciliates (<20 μm)	2660	0	0
Unid. Flag. sp. 1 (ca. 15 μm)	17 960	50 904	14 856
Cryptophyceae	9720	2832	3192
Phaeocystis sp.	1 711 920	2 200 104	1 292 232
Flow cytometry			
Het Bact[a] (10^3 cells mL^{-1})	739.36	2255.27	460.51
Syn[b] (10^3 cells mL^{-1})	15.21	0.32	6.00
Pico-euk[c] (10^3 cells mL^{-1})	5.38	12.15	1.38
Nano-euk[d] (10^3 cells mL^{-1})	1.62	0.25	0.4

For a location of the stations see Fig. 1.
[a]Heterotrophic bacteria.
[b]Synechococcus.
[c]Pico-eukaryotes.
[d]Nano-eukaryotes.

Station 1. Heterotrophic bacteria were also more abundant at Station 3 compared to the others stations.

Direct examination of live concentrated plankton samples in the field, even when using the basic microscope available, clearly indicated the presence of *Azadinium* sp. (Fig. 2A and B) in the water, as indicated by size, shape and from the characteristic swimming pattern. A characterization and quantification of the whole plankton community using fixed samples showed that gross plankton composition was fairly similar in the area (Table III), with particularly high abundances of the colonial haptophycean species *Phaeocystis* sp. In addition, the diatoms *Guinardia striata* and *G. delicatula* were high in abundance. Among dinophycean, large *Tripos* (*T. muelleri*, *T. furca*) and *Dinophysis* (*Dinophysis acuminata*, *D. caudata*) and a highly diverse community of species of the heterotrophic genus *Protoperidinium* were present. At stations 1 and 4, a number of small dinoflagellates of an "*Azadinium*-like" appearance (Fig. 2C–F) in the fixed samples were present with maximum densities of 6.8 × 10^3 cells L^{-1} (Table III).
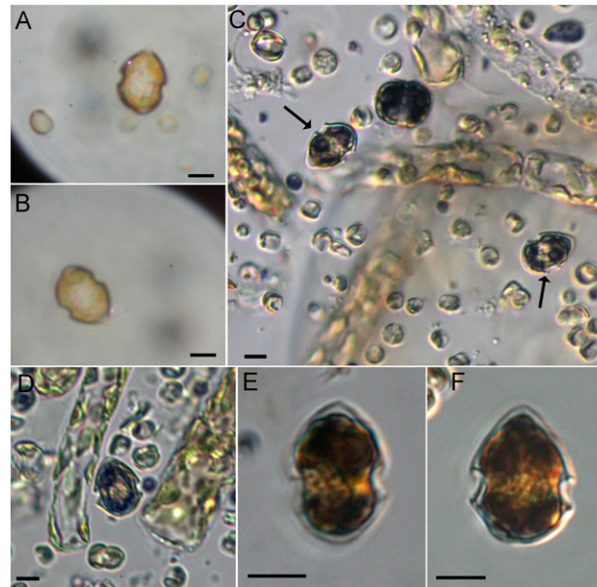
Fig. 2. Live (**A**, **B**) and lugol-fixed (**C**–**F**) field samples from station 1 showing presence of *Azadinium* sp. (A, B) and/or "*Azadinium*-like" cells (C (arrows)–F). Scale bar = 5 μm.

Molecular detection of Azadinium cells in field samples

All field samples analyzed were positive for *A. poporum* molecular detection using specific primers for this species. Neither *A. spinosum* nor *A. obesum* yielded positive signals using specific primer for these two species (data not shown).

Lipophilic toxins

None of the currently known AZA (Table II) could be detected, either in the screening of the plankton (3–20 μm size) filters or in the plankton concentrates of net hauls. However, in the plankton concentrates pectenotoxins (PTX) were present at all three stations. In the net hauls PTX-2 seco acid (PTX-2sa) was more abundant than PTX-2 with a maximum value of 779 ng PTX-2sa per net tow at Station 4 (Table I).

Azadinium poporum cultures

### Morphology, light- and electron microscopy

Inspection of living field samples and cell isolation yielded three clonal cultures (1-C11, 1-D5 and 2-B9) identified as *Azadinium*, all of them originating from Station 1. Light microscopy (LM) and SEM of isolates confirmed that they all were identical in terms of morphology and that they all represented the species *A. poporum*.

General size, cell shape, pattern and arrangement of thecal plates were consistent with previous descriptions of the species (Fig. 3). Freshly formalin preserved cells

ranged from 11.9 to 18.0 μm in length and 9.3 to 14.4 μm in width (mean ± SD length and width: 15.0 ± 1.3 μm and 11.5 ± 1.1 μm, $n = 62$ for 1-C11; 14.7 ± 1.1 μm and 11.6 ± 1.1, $n = 105$ for 1-D5; 14.7 ± 1.2 μm and 11.3 ± 1.0, $n = 86$ for 2-B9). The mean length/width ratio of all measurements of all isolates was of 1.3.

Chilean *A. poporum* were ovoid with a broad slightly descending cingulum (Fig. 3C and D). The episome was higher than the hyposome and terminated in a conspicuous apical pore complex (APC) (Fig. 3B and C). The hyposome was broadly rounded (Fig. 3A, F and G–I) or slightly dented with an irregular outline (Fig. 3 B–C).
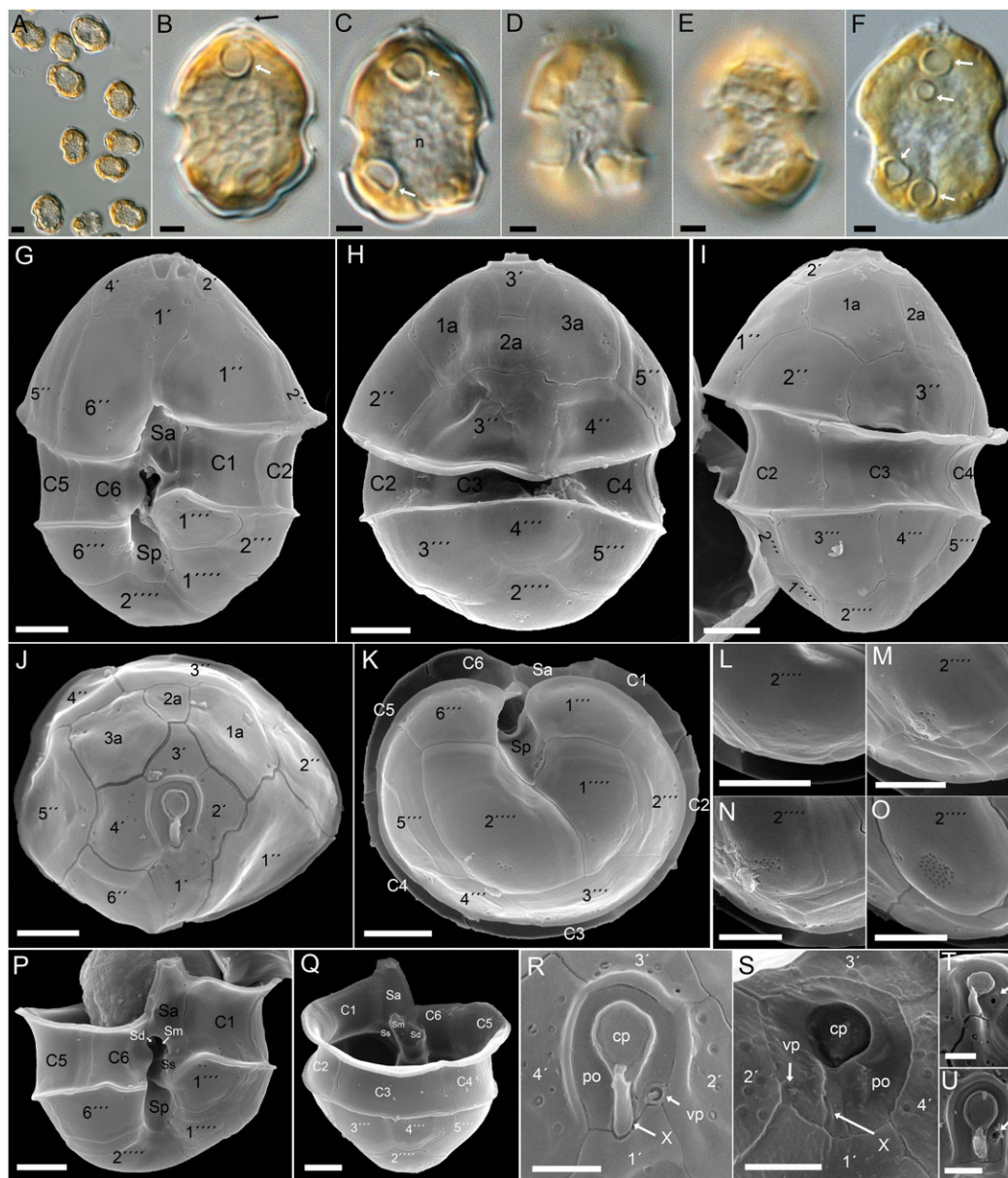
Fig. 3. *Azadinium poporum* (Chilean strains). LM (**A–F**) of formalin fixed cells or SEM (**G–U**) micrographs. (**A–F**) General size and shape. Note the presence of large pyrenoids in the episome and in the hyposome (white arrows in B, C and F). Black arrow in B indicates the pointed apical pore complex. (**D**, **E**) Same cell in ventral (D) or dorsal (E) view. In (E) note the parietally located and reticulate chloroplast. (G–U) SEM micrographs of different cells to illustrate thecal plate arrangement and plate details. Whole cell in (**G**) ventral view, (**H**) dorsal view, or (**I**) lateral view. (**J**) Epitheca in apical view. (**K**) Hypotheca in antapical view. (**L–O**) Detailed view of the field of pores on plate 2‴‴. (**P**) Ventral view of the hypotheca showing sulcal plate arrangement. (**Q**) Dorsal/apical view of the hypotheca showing the series of cingular plates (C1–C6) with an interior view of the sulcal plates. (Sa: anterior sulcal plate; Sp: posterior sulcal plate; Ss: left sulcal plate; Sm: median sulcal plate; Sd: right sulcal plate). (R, S), Apical pore complex (APC) in external (**R**) and internal (**S**) view. po = pore plate, cp = cover plate, vp = ventral pore, X = X-plate. (**T**, **U**) Two rare cases where the ventral pore (white arrow) was found slightly displaced inside of the pore plate. Scale bars = 2 μm (A–Q) or = 1 μm (R–U).

A presumably single lobed and retiform chloroplast (Fig. 3E) and a large ovoid nucleus in the center of the cell (Fig. 3C) were visible in LM. Pyrenoid(s) with a starch sheath (visible as a ring-like structure) were always present (Fig. 3B, C and F). The number of pyrenoids per cell was difficult to determine reliably but generally multiple pyrenoids were observed. Within all cells inspected pyrenoid numbers from 1 to 6 were recorded, however the most common number of pyrenoids per cell was two, one located in the epi- and hyposome, respectively (Fig. 3C).

The plate pattern (Fig. 3G–K; P–R) with the APC consisting of a pore plate, a cover plate and a small and rectangular X-plate (Fig. 3R and S), with four apical plates, three anterior intercalary plates, with six plates each in the precingular, the cingular and the postcingular series, with five sulcal plates and with two antapical plates, agreed with previous descriptions of the type material for *A. poporum* (Tillmann *et al.*, 2011) as was the size and arrangement of plates and the presence and location of the ventral pore (Fig. 3) located on the left lateral side of the pore plate.

Thecal plates were smooth and irregularly covered by few small pores. Most conspicuously, the number of thecal pores on the large right antapical plate 2′′′′ was variable within all three isolates, ranging from very few to a high number of pores forming a distinct field (Fig. 3L–O).

All three cultured strains exhibited some variability in terms of shape of plates, and a number of deviations from the typical plate pattern were observed. Variations in plate pattern primarily consisted of additional sutures between the epithecal plates, although variation in number of hypothecal plates was also observed (not shown). The position of the ventral pore was consistent among hundreds of cells inspected, but as a rare exception the pore was found slightly displaced inside of the pore plate (Fig. 3T–U).

Phylogeny

Azadinium poporum ITS and LSU sequence analyses using *A. dalianense* as outgroup show similar results, both for ML and Bayesian inference phylogenies. ITS and LSU rDNA phylogenetic analysis indicated that Chilean *A. poporum* strains cluster together with strains from the North Sea, and Tasmanian Sea, in well-supported clades. The best scoring ML trees for ITS and LSU rDNA genes (−ln = 1292.77 and 1266.23, respectively) are shown in Fig. 4 and 5, in which most nodes had high statistical support. In the case of the ITS based phylogeny, high bootstrap and probability values strongly supported that *A. poporum* 2-B9, 1-C11 and 1-D5 are part of the ribotype A of *A. poporum* (ML bootstrap support value, ML-BS: 93 and Bayesian posterior probability value, B-PP: 1). This was also inferred using the LSU sequences, Chilean *A. poporum* form a highly supported clade containing the

isolates from the North Sea and *A. poporum* CAWD230 from Tasmanian Sea (ML-BS: 98, B-PP: 0.99). Overall topology using ITS (Fig. 4) and LSU rDNA genes (Fig. 5) shows 3 well-supported clades, comprising the *A. poporum* ribotypes A, B and C, with the isolate from the Gulf of Mexico clustering outside ribotypes B and C, within not well resolved branches (ribotype D). Clades corresponding for ribotypes B and C (ML-BS: 86, B-PP: 0.48, and ML-BS: 96, B-PP:1, for ITS and ML-BS: 89, B-PP: 0.99, and ML-BS: 84, B-PP: 0.89 for LSU, respectively), were highly consistent between them.

For the ITS sequences, multiple sequence global alignment indicates that Chilean *Azadinium* strains are 99.8% similar with a 629 bp comparison, and only one mismatch. Visual inspection of the Sanger spherogram indicated that this mismatch is not due to sequencing error. Similarity inside the different ribotypes of *A. poporum* ranged from 99.4 to 98.6%, for ribotypes A and C, and B, respectively. Inside the ribotype A, two mismatch or variable positions differentiate the strains from the Southeast Pacific, off Chile from the ones from the North Sea, off Denmark. For the LSU rDNA gene, Chilean *Azadinium* strains are 100% similar along 650 bp. Similarity inside the different ribotypes was 99.8, 98 and 99.7% for ribotype A, B and C, respectively. For the ribotype A, only one variable position separates Chilean strains (Southeast Pacific) and the one from New Zealand (Tasmanian Sea), from the European (North Sea). Tables IV and V show pairwise comparisons of partial ITS and LSU sequences of selected strains from each ribotype of *A. poporum*, including the ribotype D, with only one representative, GM29 from the Gulf of Mexico. A higher variability can be seen in the LSU rDNA gene fragments, as represented by the high number of variable positions and lesser similarity compared to the ITS rDNA fragment.

Azaspiracids

All three Chilean isolates of *A. poporum* displayed qualitatively identical AZA profiles. The profiles consisted of AZA-11 as the most abundant variant followed by AZA-11 phosphate (*m/z* 952) and by another phosphorylated AZA with a *m/z* value of 910. AZA-11 was unambiguously identified by comparison of retention times and collision induced dissociation (CID) spectra of the sample (Fig. 6A) with AZA-11 isolated and purified from Irish mussels. AZA-11 phosphate was identified by its CID spectrum, which showed the identical fragments of AZA-11, but which were generated from the 80 Da higher pseudo-molecular ion *m/z* 952 (Fig 6B). In addition to these two AZA, a third AZA-related compound (1) with *m/z* 910 was detected by a precursor scan of *m/z* 362. This compound has not been reported before, but shows all characteristic AZA fragments in its CID spectrum: *m/z*

Fig. 4. Maximum likelihood tree based on ITS sequences from the *Azadinium poporum* strains. The tree was rooted using *Azadinium dalianense* AZCH02. The alignment comprised 43 sequences, with 620 informative positions. Numbers above or below branches represent ML bootstrap support values/Bayesian posterior probability values, only ≥0.90, and ≥50 are shown. Scale bars indicate number of nucleotide substitutions per site. *A. poporum* strains from the Southeast Pacific, off Chile, characterized in this study are shown in bold.

462, 362, 262 and 168 (Fig. 6C). Like AZA-11 phosphate, the spectrum of (1) shows no fragments between m/z 910 and 830, which leads to the conclusion that (1) likewise is a phosphorylated AZA.

Spike experiment In order to test if AZA-11 phosphate was an extraction artefact or *de novo* synthesized by *A. poporum*, in separate experiments AZA-1 and AZA-2, respectively, were added to cell pellets of *A. poporum*
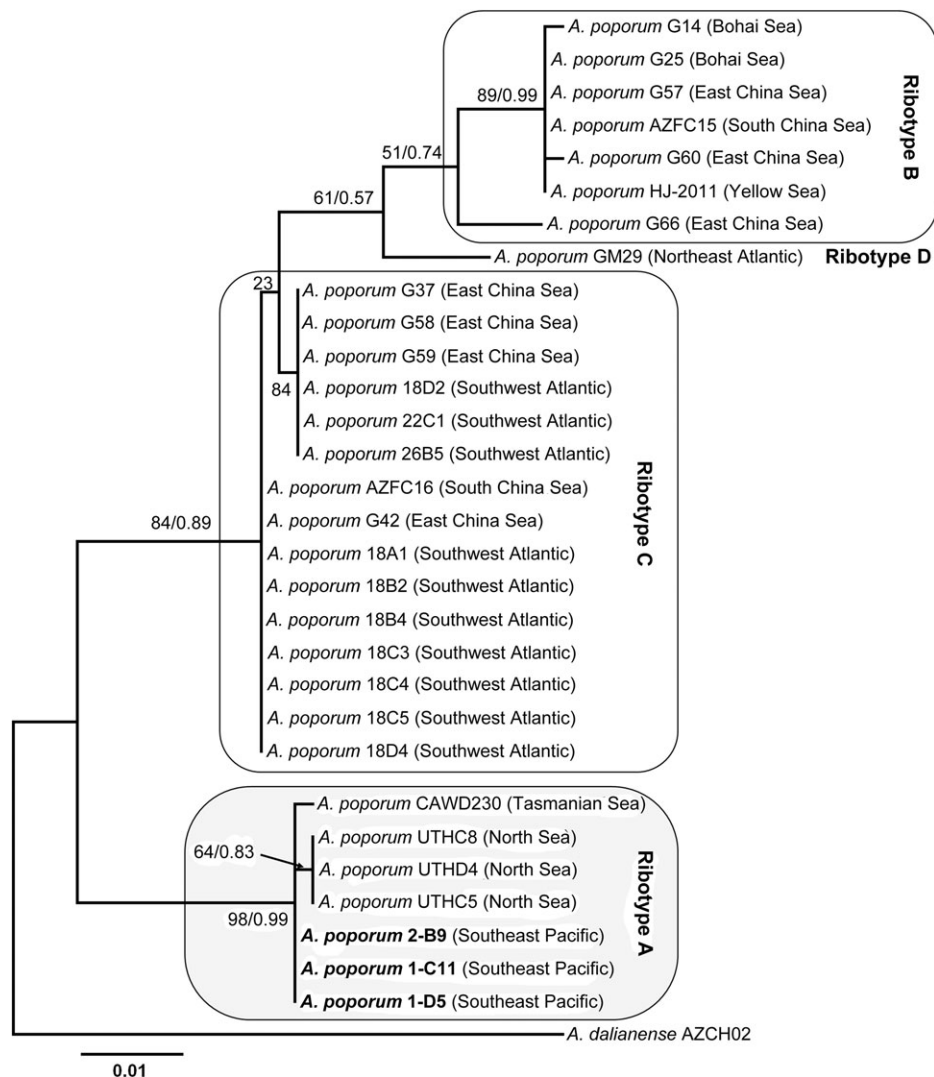
Fig. 5. Maximum likelihood tree based on LSU rDNA gene sequences from the *Azadinium poporum* strains. The tree was rooted using *Azadinium dalianense* AZCH02. The alignment comprised 31 sequences, with 617 informative positions. Numbers above or below branches represent ML bootstrap support values/Bayesian posterior probability values, only ≥0.90, and ≥50 are shown. Scale bars indicate number of nucleotide substitutions per site. *A. poporum* strains from the Southeast Pacific, off Chile, characterized in this study are shown in bold.

Table IV: Pairwise genetic similarity (%) of partial ITS rDNA fragments between selected A. poporum strains from each ribotype and number of variable positions (in parenthesis)

	A		B		C		D
Ribotype	Southeast Pacific 1-D5	North Sea UTHC5	Bohai Sea G25	East China Sea G62	East China Sea G42	Southwest Atlantic 18A1	Gulf of Mexico GM29
1-D5		99.7 (2)	97.5 (16)	97.6 (15)	97.5 (16)	97.8 (14)	97.8 (14)
UTHC5			97.4 (17)	97.5 (16)	97.4 (16)	97.5 (15)	97.6 (14)
G25				99.8 (1)	98.3 (11)	98.1 (12)	98.9 (7)
G62					98.1 (12)	98.0 (13)	98.8 (8)
G42						99.5 (3)	98.4 (10)
18A1							98.3 (11)

Table V: Pairwise genetic similarity (%) of partial LSU rDNA fragments between selected A. poporum strains from each ribotype and number of variable positions (in parenthesis)

Ribotype	A			B	C		D
	Southeast Pacific 1-D5	North Sea UTHC5	Tasmanian Sea CAWD230	Bohai Sea G25	East China Sea G42	Southwest Atlantic 18A1	Gulf of Mexico GM29
1-D5		99.8 (1)	100 (0)	96.0 (26)	96.3 (24)	96.3 (23)	95.1 (31)
UTHC5			99.9 (1)	96.5 (26)	96.8 (23)	96.5 (22)	95.5 (32)
CAWD230				96.3 (25)	96.6 (24)	96.3 (24)	95.9 (32)
G25					97.8 (16)	97.7 (16)	97.7 (16)
G42						100 (0)	98.3 (12)
18A1							98.2 (12)

1-C11 prior to AZA extraction. After extraction both samples were tested for their AZA profiles. Whereas AZA-11 and AZA-11 phosphate were detected in both experiments, no phosphates of AZA-1 and AZA-2 were detected in any experiment (data not shown).

Cell quota AZA-11 cell quota as AZA-1 equivalents were estimated from four independently grown cultures each and were 3.2 ± 0.9, 3.1 ± 0.7 and 3.6 ± 2.8 pg cell^{-1} for isolate 1-C11, 1-D5 and 2-B9, respectively. AZA-11 phosphate was less abundant in these strains. The highest proportion of the phosphate was found in strain 1-C11 with 13%, whereas strains 1-D5 and 2-B9 had 7 and 4% of AZA-11, respectively. Even less abundant was compound (1) with 0.4, 0.7 and 0.3% of AZA-11 in strains 1-C11, 1-D5 and 2-B9, respectively.

DISCUSSION

This is the first record of the toxic genus *Azadinium* and of the species *A. poporum* in waters from the Pacific side of South America. *Azadinium poporum* was initially described from the North Sea (Tillmann *et al.*, 2011) as the third description of a species within this genus. Since then it has been identified in various areas such as the Asian Pacific (Potvin *et al.*, 2012; Gu *et al.*, 2013), New Zealand (Smith *et al.*, 2016), Gulf of Mexico (Luo *et al.*, 2016) or South Atlantic of Argentina (Tillmann *et al.*, 2016). This first record of *A. poporum* from Chile represents an important range extension of the species to the Southeastern Pacific and thus confirms that this species has a rather widespread global distribution. *Azadinium poporum* requires special attention because this is one of the four species of Amphidomataceae that produce the human gastrointestinal toxin AZA.

Morphology

Both morphology and phylogeny leave no doubt that all three Chilean *Azadinium* strains indeed can be identified as *A. poporum*. At the LM level, general size and shape as well as the presence of multiple pyrenoids with a starch sheath (visible as a ring-like structure) agree with the type material of *A. poporum*. Plate details most important for identification of *Azadinium* species include the presence/absence and/or location of a single antapical spine and primarily the position of a ventral pore (Tillmann *et al.*, 2014a, 2014b). The Chilean strains show the ventral pore position typical for *A. poporum* being located anterior at the cells left side of the pore plate at the junction with the first two apical plates. A rather similar position of the ventral pore, however, is also present in *Azadinium dalianense* and *Azadinium trinitatum* (Luo *et al.*, 2013; Tillmann *et al.*, 2014a). *Azadinium dalianense* differ significantly in number of apical plates (Luo *et al.*, 2013; Tillmann and Akselman, 2016). *Azadinium trinitatum* has an antapical spine, and the position of the ventral pore is slightly different; whereas the ventral pore is located more in a cavity of the pore plate in *A. poporum*, the ventral pore in *A. trinitatum* is located more in a cavity of the 1′ plate at the tip of an elongated side of the pore plate. Despite some variability in general shape, the Chilean strains did not show a variability in hypothecal shape as described for the Argentinean strains of *A. poporum* (Tillmann *et al.*, 2016). In contrast, a structured field of pores on the second apical plate, which was emphasised as a conspicuous feature of Argentinean *A. poporum*, was also seen for some cells of the Chilean strains, but the number of pores in this area was highly variable (Fig. 4L–O). Such a group of pores on the dorsal side of the second antapical plate was also occasionally observed in *A. poporum* from the Gulf of Mexico (Luo *et al.*, 2016), in a Korean strain (Potvin *et al.*, 2012), and in many Chinese strains (Haifeng Gu, personal communication). This suggests that this is a widespread and common morphological feature of *A. poporum*, which however seems not to be stable and thus is of little diagnostic value. As it has been described for other *A. poporum* cultures (Tillmann *et al.*, 2011; Gu *et al.*, 2013; Luo *et al.*, 2016; Tillmann *et al.*, 2016), aberrant plate pattern
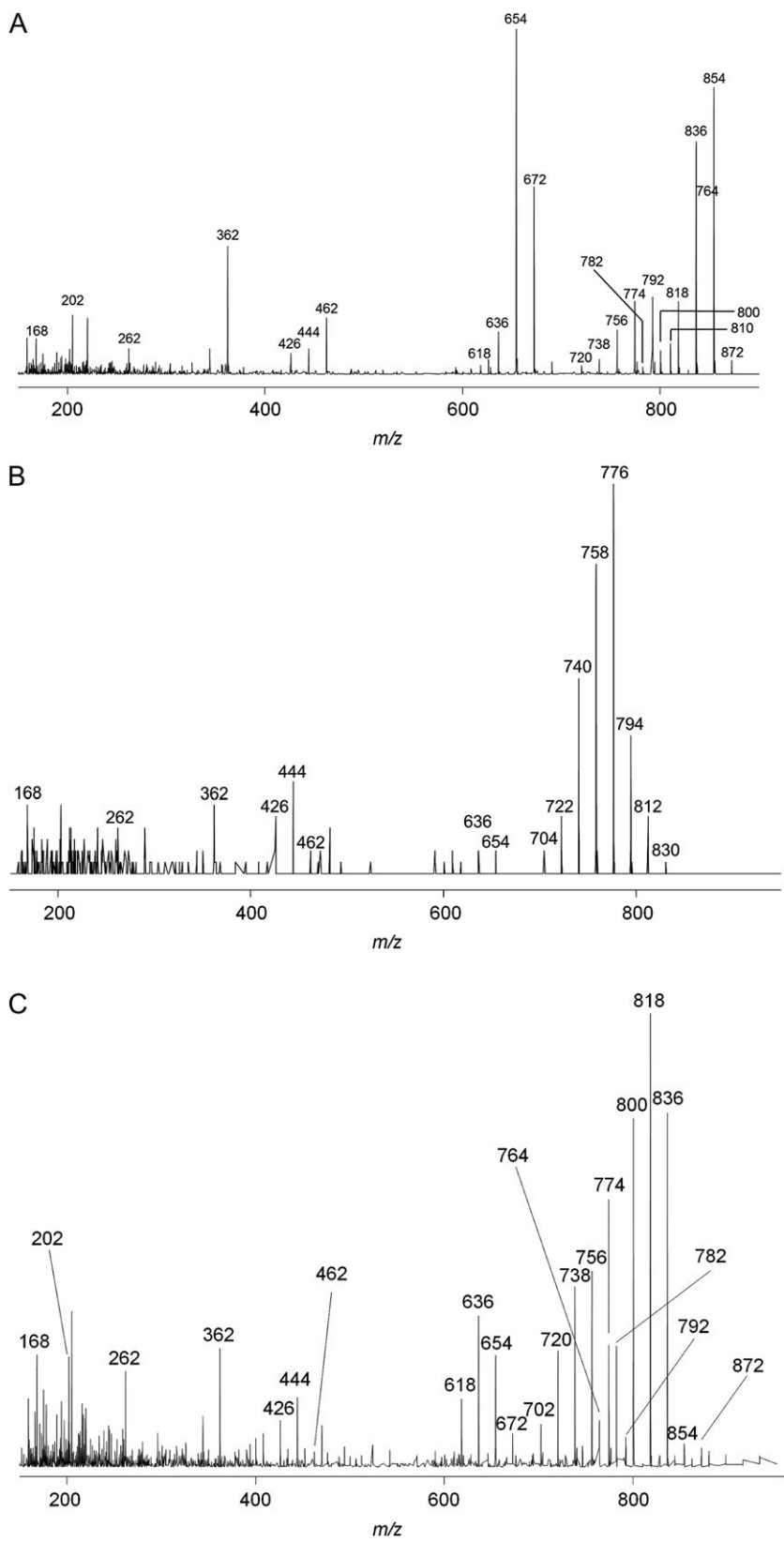
Fig. 6. CID spectrum of (**A**) AZA-11, (**B**) AZA-11 phosphate and (**C**) AZA-910.

also occurred in cultures of the Chilean strains of *A. poporum*. The position of the ventral pore, however, was rather stable and supports the view that this is a distinct and species-specific character for species of *Azadinium*, although very rarely deviating positions of the ventral pore, as detected here for two cells (Fig. 3T and U) were recorded for other strains/species as well (Potvin *et al.*, 2012; Tillmann *et al.*, 2014a).

Phylogeny

Molecular phylogeny likewise shows that the Chilean *Azadinium* strains belong to *A. poporum*. As in all previous ITS/LSU trees of *A. poporum* strains (Gu *et al.*, 2013; Luo *et al.*, 2016; Tillmann *et al.*, 2016), *A. poporum* forms well-supported clades, one of them (ribotype B) including multiple strains originating from the coast of China as well as the Korean strain. A second clade (ribotype C) includes strains from the East China Sea, South China Sea and the Argentinean strains; and a third (ribotype A) consists of strains from Europe, the strain from New Zealand, and all three Chilean strains. Slight differences in the position of some strains from the ribotypes B and C between this work, Gu *et al.* (2013), Tillmann *et al.* (2016) and Luo *et al.* (2016), reinforce the need for more isolates to capture a more accurate picture of the genetic variation inside the *A. poporum* species. More importantly, valid biogeographic inferences probably will require not only a much larger number of isolates, but also a much wider geographical coverage. Moreover, analysis of other more variable marker genes would be needed for a detailed investigation of genetic diversity and distribution inside the *Azadinium* genus. Nevertheless, available data suggest that South Atlantic (Argentina) and North Pacific (Korea, China) strains on one hand, and South Pacific strains from both New Zealand and Chile together with European strains seem to originate from a single ancestor and that dispersal links should exist between these distant geographical areas.

Field situation

Chañaral area at northern Chile is characterized on one hand by important anthropogenic pollution due to continuous mine tailings discharging that deposited around 280×10^6 tons of untreated copper residues (Correa *et al.*, 1999). On the other hand, the area encompasses a large National Park including one of the most important marine fauna reservoirs in the Humboldt Current System. *Azadinium poporum* was observed in the area in full saline (salinity 34.5) conditions and rather cold water temperature 12–14 °C. Waters were characterized by a N:P ratio below the Redfield's value (Redfield, 1958), and similar values of N and Silicates, as reflected in the Redfield ratio for diatoms (Brzezinski, 1985). Specimens of *A. poporum* were part of a community quite typical for late summer plankton dominated by diatoms and the haptophyte *Phaeocystis* sp. and with *Dinophysis acuminata* and the *Dinophysis* toxins present. Identifying the presence of *Azadinium* in live samples was straightforward, as here the typical swimming pattern could be used as a distinctive feature in addition to cell size and shape. In the Lugol fixed samples it was more difficult to differentiate *Azadinium* from similar sized species (e.g. *Heterocapsa* spp.). The abundance data are therefore given as "*Azadinium*-like cells" and thus are most probably overestimating true *Azadinium* abundance. In any case, a maximum value of 6800 cells L^{-1} of *Azadinium*-like cells indicates that abundance was low compared to bloom densities of *Azadinium* reported in Argentina of 2.5×10^6 cell L^{-1} (Akselman and Negri, 2012). This corresponds to the fact that AZA were not chemically detected in the Chañaral samples. Exclusive of any potential loss of toxins due to the filtration method, according to the detection limit of the LC–MS method, combined with the sample and extraction volume and a cell quota of 3.3 fg cell^{-1}, a positive AZA record would have required a minimum concentration of 8000 cells L^{-1}. Nevertheless, the presence of *A. poporum* in the area was confirmed by positive signals of the *A. poporum* specific molecular marker. PCR detection for two other species of *Azadinium*, *A. spinosum* and *A. obesum*, were negative, however it cannot be excluded that these species occur at a different time in the year or in other locations along the Chilean coast. Likewise, obtaining three isolates of the same species does not mean that other species of *Azadinium* are absent. AZA-1 has been detected in Chilean shellfish samples (Álvarez *et al.*, 2010; López-Rivera *et al.*, 2010), and this compound has up to now not been found for *A. poporum*, providing evidence for the presence of other species of Amphidomataceae in this region. In contrast, AZA-11, the compound produced by Chilean *A. poporum*, has not been reported in previous shellfish analysis, but this can be explained because the methods used in the above mentioned works by López-Rivera *et al.* (2010) and Álvarez *et al.* (2010) were not designed to detect AZA-11.

Toxins

For the Chilean strains of *A. poporum* the analysis revealed only one AZA, namely AZA-11. This AZA derivative, even though initially reported as a shellfish metabolite of AZA-2 through 3-hydroxylation (Rehmann *et al.*, 2008) has been reported before to be produced by several strains of *A. poporum* from the Northwest Pacific (Krock *et al.*,

2014). Nevertheless, toxin profile variability of *A. poporum* seems to be high in the Northwest Pacific with *A. poporum* strains producing AZA-2, -11, -36, -40 and -41 (Krock *et al.*, 2014). The strains from Chile reported here produce only AZA-11, but these are the only strains from the Southeast Pacific available so far. Available strains of *A. poporum* from the other side of the South American continent, in the Southwest Atlantic, also produce only one AZA, which is AZA-2 (Tillmann *et al.*, 2016). Altogether, these data point to the need of further studies for both sides of South America to fully evaluate whether this situation reflects a conserved toxin profile representative for a larger area. Within Argentinean *A. poporum* for the first time a phosphorylated variant of AZA-2 has been reported (Tillmann *et al.*, 2016), which prompted us to investigate, if the Chilean isolates of *A. poporum* also contained the respective phosphate. This was indeed found and raises the question, if the AZA phosphates are true dinoflagellate secondary metabolites or if phosphorylation is an extraction artefact which might occur during spontaneous or enzymatic reaction during cell homogenization. In order to test this hypothesis a spike experiment was performed in which AZA-1 and AZA-2 were added to *A. poporum* cell pellets before homogenization of the sample and to test if phosphates of these two AZA were formed during extraction. However, this was not the case. In contrast to the presence of AZA-11 phosphate, no AZA-1 or AZA-2 phosphates were detected. This leads to the conclusion that AZA phosphorylation is occurring *de novo* within the dinoflagellate cells. Interestingly, the *A. poporum* isolates, in addition to AZA-11 and its phosphate, produce another AZA-related compound with pseudomolecular ion m/z 910. Its CID spectrum (Fig. 6C) would be consistent with AZA-35 which has recently been described by Kilcoyne *et al.* (2014) from *A. spinosum*. However, the corresponding parent compound AZA-35 or any other AZA with this m/z value could not be detected in these strains. This was quite unexpected, as in the case of AZA-11 the phosphate showed much smaller abundances as the parent compound AZA-11. The same was also observed for the Argentinean strain of *A. poporum* (Tillmann *et al.*, 2016), where the parent compound AZA-2 was much more abundant than its phosphate. At the moment there is no explanation for this discrepancy, but it may be an indication that AZA biosynthesis or internal turnover is more complex than currently believed.

CONCLUSION

The *A. poporum* strains from the Southeast Pacific characterized in this work underline the cosmopolitan distribution of this species. Toxin production and molecular phylogeny indicate that the Chilean *A. poporum* strains share AZA-11 production with some Asian strains, but are genetically similar to the Northern Europe isolates, suggesting that these strains emerged from a single ancestor and that dispersal links should exist between these distant geographical areas. This first confirmation of the presence of AZA producing *Azadinium* in the Chilean coastal area underlines the risk of AZA shellfish and concomitant human contamination episodes in the Southeastern Pacific region.

SUPPLEMENTARY DATA

Supplementary data are available at *Journal of Plankton Research* online.

ACKNOWLEDGEMENTS

FUNDING

REFERENCES

Adachi, M., Sako, Y. and Ishida, Y. (1996) Analysis of *Alexandrium* (Dinophyceae) species using sequences of the 5.8S ribosomal DNA and internal transcribed spacer regions. *J. Phycol.*, **32**, 424–432.

Akselman, R. and Negri, R. M. (2012) Blooms of *Azadinium* cf. *spinosum* Elbrächter et Tillmann (Dinophyceae) in northern shelf waters of Argentina, Southwestern Atlantic. *Harmful. Algae*, **19**, 30–38.

Akselman, R., Negri, R. M. and Cozzolino, E. (2014) *Azadinium* (Amphidomataceae, Dinophyceae) in the Southwest Atlantic: *in situ* and satellite observations. *Rev. Biol. Mar. Oceanogr.*, **49**, 511–526.

Alheit, J. and Bernal, P. A. (1993) Effects of physical and biological changes on the biomass yield of the Humboldt Current System. In Sherman, K., Alexander, L. M. and Gold, B. D. (eds.), *Large Marine Ecosytems*. American Association for the Advancement of Science Press, Washington, DC, pp. 53–68.

Álvarez, G., Uribe, E., Ávalos, P., Mariño, C. and Blanco, J. (2010) First identification of azaspiracid and spirolides in *Mesodesma donacium* and *Mulinia edulis* from Northern Chile. *Toxicon*, **55**, 638–641.

Álvarez, G., Uribe, E., Díaz, R., Braun, M., Mariño, C. and Blanco, J. (2011) Blooms of the Yessotoxin producing dinoflagellate *Protoceratium reticulatum* (Dinophyceae) in Northern Chile. *J. Sea Res.*, **65**, 427–434.

Álvarez, G., Uribe, E., Vidal, A., Ávalos, P., Gonzáles, F., Marina, C. and Blanco, J. (2009) Paralytic shellfish toxins in *Argopecten purpuratus* and *Semimytilus algosus* from northern Chile. *Aquat. Living Resour.*, **22**, 341–347.

Amzil, Z., Sibat, M., Royer, F. and Savar, V. (2008) First report on azaspiracid and yessotoxin groups detection in French shellfish. *Toxicon*, **52**, 39–48.

Blanco, J., Álvarez, G. and Uribe, E. (2007) Identification of pectenotoxins in plankton, filter feeders, and isolated cells of a *Dinophysis acuminata* with an atypical toxin profile, from Chile. *Toxicon*, **49**, 710–716.

Braña Magdalena, A., Lehane, M., Krys, S., Fernández, M. L., Furey, A. and James, K. J. (2003) The first identification of azaspiracids in shellfish from France and Spain. *Toxicon*, **42**, 105–108.

Brzezinski, M. A. (1985) The Si:C:N ratio of marine diatoms: interspecific variability and the effect of some environmental variables. *J. Phycol.*, **21**, 347–357.

Correa, J. A., Castilla, J. C., Ramírez, M., Varas, M., Lagos, N., Vergara, S., Moenne, A., Román, D. *et al.* (1999) Copper, copper mine tailings and their effect on marine algae in Northern Chile. *J. Appl. Phycol.*, **11**, 57–67.

Daneri, G., Dellarossa, V., Quinones, R., Jacob, B., Montero, P. and Ulloa, O. (2000) Primary production and community respiration in the Humboldt Current system off Chile and associated oceanic areas. *Mar. Ecol. Prog. Ser.*, **197**, 41–49.

Edgar, R. C. (2004) MUSCLE: multiple sequence alignment with high accuracy and high throughput. *Nucl. Acids Res.*, **32**, 1792–1797.

Felsenstein, J. (1981) Evolutionary trees from DNA sequences: a maximum likelihood approach. *J. Mol. Evol.*, **17**, 368–376.

Fuhrman, J. A., Comeau, D. E., Hagström, Å. and Chan, A. M. (1988) Extraction from natural planktonic microorganisms of DNA suitable for molecular biological studies. *Appl. Environ. Microbiol.*, **54**, 1426–1429.

García-Mendoza, E., Sánchez-Bravo, Y. A., Turner, A., Blanco, J., O'Neil, A., Mancera-Flores, J., Pérez-Brunius, P., Rivas, D. *et al.* (2014) Lipophilic toxins in cultivated mussels (*Mytilus galloprovincialis*) from Baja California, Mexico. *Toxicon*, **90**, 111–123.

Gelcich, S., Hughes, T. P., Olsson, P., Folke, C., Defeo, O., Fernández, M., Foale, S., Gunderson, L. H. *et al.* (2010) Navigating transformations in governance of Chilean marine coastal resources. *Proc. Natl. Acad. Sci. USA*, **107**, 16794–16799.

Gu, H., Luo, Z., Krock, B., Witt, M. and Tillmann, U. (2013) Morphology, phylogeny and azaspiracid profile of *Azadinium poporum* (Dinophyceae) from the China Sea. *Harmful Algae*, **21–22**, 64–75.

Guzmán, L., Pacheco, H., Pizarro, G. and Alarcón, C. (2002) *Alexandrium catenella* y veneno paralizante de los mariscos en Chile. In Sar, E., Ferrario, M. E. and Reguera, B. (eds.), *Floraciones Algales Novicas en el Cono Sur Americano*. Instituto Espanol de Oceanographia Espana, Vigo, Spain, pp. 237–256.

Hallegraeff, G. (2014) Harmful algae and their toxins: progress, paradoxes and paradigm shifts. In Rossini, G. P. (ed.), *Toxins and Biologically Active Compounds from Microalgae*, **Vol. 1**, CRC Press, Boca Raton, pp. 3–20.

Hallegraeff, G. M. (2003) Harmful Algal Blooms: a global overview. In Hallegraeff, G. M., Anderson, D. and Cembella, A. D. (eds.), *Manual on Harmful Marine Microalgae*. Paris, pp. 25–49.

Hernández-Becerril, D. U., Barón-Campis, S. A. and Escobar-Morales, S. (2012) A new record of *Azadinium spinosum* (Dinoflagellata) from the tropical Mexican Pacific. *Rev. Biol. Mar. Oceanogr.*, **47**, 553–557.

Huelsenbeck, J. and Ronquist, F. (2001) MRBAYES: Bayesian inference of phylogenetic trees. *Bioinformatics.*, **17**, 754–755.

Iriarte, J. L. and González, H. E. (2004) Phytoplankton size structure during and after the 1997/89El Nino in a coastal upwelling area of the northern Humboldt Current System. *Mar. Ecol. Prog. Ser.*, **269**, 83–90.

James, K. J., Furey, A., Lehane, M., Ramstad, H., Aune, T., Hovgaard, P., Morris, P., Higman, W. *et al.* (2002) First evidence of an extensive northern European distribution of azaspiracid poisoning (AZP) toxins in shellfish. *Toxicon*, **40**, 909–915.

Keller, M. D., Selvin, R. C., Claus, W. and Guillard, R. R. L. (1987) Media for the culture of oceanic ultraphytoplankton. *J. Phycol.*, **23**, 633–638.

Kilcoyne, J., Nulty, C., Jauffrais, T., McCarron, P., Herve, F., Foley, B., Rise, F., Crain, S. *et al.* (2014) Isolation, structure elucidation, relative LC-MS response, and in vitro toxicity of azaspiracids from the dinoflagellate *Azadinium spinosum*. *J. Nat. Prod.*, **77**, 2465–2474.

Kimura, M. (1980) A simple method for estimating evolutionary rate of base substitutions through comparative studies of nucleotide sequences. *J. Mol. Evol.*, **16**, 111–120.

Krock, B., Seguel, C. G., Valderrama, K. and Tillmann, U. (2009a) Pectenotoxins and yessotoxin from Arica Bay, North Chile as determined by tandem mass spectrometry. *Toxicon*, **54**, 364–367.

Krock, B., Tillmann, U., John, U. and Cembella, A. D. (2008) LC–MS/MS on board ship—tandem mass spectrometry in the search for phycotoxins and novel toxigenic plankton from the North Sea. *Anal. Bioanal. Chem.*, **392**, 797–803.

Krock, B., Tillmann, U., John, U. and Cembella, A. D. (2009b) Characterization of azaspiracids in plankton size-fractions and isolation of an azaspiracid-producing dinoflagellate from the North Sea. *Harmful Algae*, **8**, 254–263.

Krock, B., Tillmann, U., Voß, D., Koch, B. P., Salas, R., Witt, M., Potvin, E. and Jeong, H. J. (2012) New azaspiracids in Amphidomataceae (Dinophyceae): proposed structures. *Toxicon*, **60**, 830–839.

Krock, B., Tillmann, U., Witt, M. and Gu, H. (2014) Azaspiracid variability of *Azadinium poporum* (Dinophyceae) from the China Sea. *Harmful Algae*, **36**, 22–28.

Lagos, N. (1998) Microalgal blooms: a global issue with negative impact in Chile. *Biol. Res.*, **31**, 375–386.

López-Rivera, A., O'Callaghan, K., Moriarty, M., O'Driscoll, D., Hamilton, B., Lehane, M., James, K. J. and Furey, A. (2010) First evidence of azaspiracids (AZAs): a family of lipophilic polyether marine toxins in scallops (*Argopecten purpuratus*) and mussels (*Mytilus chilensis*) collected in two regions of Chile. *Toxicon*, **55**, 692–701.

Luo, Z., Gu, H., Krock, B. and Tillmann, U. (2013) *Azadinium dalianense*, a new dinoflagellate from the Yellow Sea, China. *Phycologia*, **52**, 625–636.

Luo, Z., Krock, B., Mertens, K. N., Price, A. M., Turner, R. E., Rabalais, N. N. and Gu, H. (2016) Morphology, molecular phylogeny and azaspiracid profile of *Azadinium poporum* (Dinophyceae) from the Gulf of Mexico. *Harmful Algae*, **55**, 56–65.

Massucatto, A., Siqueira Pilotto, A. L. and Schramm, M. A. (2014) *Investigação da presença de Azaspirácidos em recursos pesqueiros do Canal do Linguado*. ISSN 2357-836X. SEPEI, Instituto Federal, Santa Catarina.

Ochoa, N., Taylor, M. H., Purca, S. and Ramos, E. (2010) Intra- and interannual variability of nearshore phytoplankton biovolume and community changes in the northern Humboldt Current system. *J. Plankton Res.*, **32**, 843–855.

Percopo, I., Siano, R., Rossi, R., Soprano, V., Sarno, D. and Zingone, A. (2013) A new potentially toxic *Azadinium* species (Dinophyceae) from the Mediterranean Sea, *A. dexteroporum* sp. nov. *J. Phycol.*, **49**, 950–966.

Potvin, É., Jeong, H. J., Kang, N. S. T., Tillmann, U. and Krock, B. (2012) First report of the photosynthetic dinoflagellate genus *Azadinium* in the Pacific Ocean: morphology and molecular characterizationof *Azadinium* cf. *poporum*. *J. Eukaryot. Microbiol.*, **59**, 145–156.

Redfield, A. C. (1958) The biological control of chemical factors in the environment. *Am. Sci.*, **46**, 205–221.

Rehmann, N., Hess, P. and Quilliam, M. A. (2008) Discovery of new analogs of the marine biotoxin azaspiracid in blue mussels *Mytilus edulis* by ultra-performance liquid chromatography/tandem mass spectrometry. *Rap. Commun. Mass Spektrom.*, **22**, 549–558.

Scholin, C. A., Herzog, M., Sogin, M. and Anderson, D. M. (1994) Identification of group- and strain-specific genetic markers for globally distributed *Alexandrium* (Dinophyceae). II. Sequence analysis of a fragment of the LSU rRNA gene. *J. Phycol.*, **30**, 999–1011.

Smayda, T. J. (1997) Harmful algal blooms: their ecophysiology and general relevance to phytoplankton blooms in the sea. *Limnol. Oceanogr.*, **42**, 1137–1153.

Smith, K. F., Rhodes, L., Harwood, D. T., Adamson, J., Moisan, C., Munday, R. and Tillmann, U. (2016) Detection of *Azadinium poporum* in New Zealand: the use of molecular tools to assist with species isolations. *J. Appl. Phycol.*, **28**, 1125–1132.

Suárez-Isla, B. A., López-Rivera, A., Hernández, C., Clement, A. and Guzmán, L. (2002) Impacto económico de las florciones de microalgas novicas en Chile y datos recientes sobre la ocurrencia de veneno amnésico de los mariscos. In Sar, E., Ferrario, M. E. and Reguera, B. (eds.), *Floraciones Algales Novicas en el Cono Sur Americano*. Instituto Espanol de Oceanographia, Vigo, Spain, pp. 257–268.

Taleb, H., Vale, P., Amanhir, R., Benhadouch, A., Sagou, R. and Chafik, A. (2006) First detection of azaspiracids in mussels in north west Africa. *J. Shellfish Res.*, **25**, 1067–1070.

Tamura, K., Stecher, G., Peterson, D., Filipski, A. and Kumar, S. (2013) MEGA6: molecular evolutionary genetics analysis version 6.0. *Mol. Biol. Evol.*, **30**, 2725–2729.

Tillmann, U. and Akselman, R. (2016) Revisiting the 1991 algal bloom in shelf waters off Argentina: *Azadinium luciferelloides* sp. nov. (Amphidomataceae, Dinophyceae) as the causative species in a diverse community of other amphidomataceans. *Phycol. Res.*, **64**, 160–175.

Tillmann, U., Borel, M., Barrera, F., Lara, R., Krock, B., Almandoz, G. and Trefault, N. (2016) *Azadinium poporum* (Dinophyceae) from

the South Atlantic off the Argentinean coast produce AZA-2. *Harmful. Algae*, **51**, 40–55.

Tillmann, U., Elbrächter, M., John, U. and Krock, B. (2011) A new non-toxic species in the dinoflagellate genus *Azadinium*: *A. poporum* sp. nov. *Eur. J. Phycol.*, **46**, 74–87.

Tillmann, U., Elbrächter, M., Krock, B., John, U. and Cembella, A. (2009) *Azadinium spinosum* gen. et sp. nov. (Dinophyceae) identified as a primary producer of azaspiracid toxins. *Eur. J. Phycol.*, **44**, 63–79.

Tillmann, U., Gottschling, M., Nézan, E., Krock, B. and Bilien, G. (2014a) Morphological and molecular characterization of three new *Azadinium* species (Amphidomataceae, Dinophyceae) from the Irminger Sea. *Protist*, **165**, 417–444.

Tillmann, U., Salas, R., Gottschling, M., Krock, B., O´Driscoll, D. and Elbrächter, M. (2012) *Amphidoma languida* sp. nov. (Dinophyceae) reveals a close relationship between *Amphidoma* and *Azadinium*. *Protist*, **163**, 701–719.

Tillmann, U., Salas, R., Jauffrais, T., Hess, P. and Silke, J. (2014b) AZA: the producing organisms—biology and trophic transfer. In Botana, L. M. (ed.), *Seafood and Freshwater Toxins*. CRC Press, Boca Raton, USA, pp. 773–798.

Toebe, K., Joshi, A. R., Messtorff, P., Tillmann, U., Cembella, A. and John, U. (2013) Molecular discrimination of taxa within the dinoflagellate genus *Azadinium*, the source of azaspiracid toxins. *J. Plankton Res.*, **35**, 225–230.

Trainer, V. L., Moore, L., Bill, B. D., Adams, N. G., Harrington, N., Borchert, J., Da Silva, D. A. M. and Eberhard, B. T. L. (2013) Diarrhetic shellfish toxins and other lipophilic toxins of human health concern in Washington State. *Mar. Drugs*, **11**, 1815–1835.

Trefault, N., Krock, B., Delherbe, N., Cembella, A. and Vásquez, M. (2011) Latitudinal transects in the southeastern Pacific Ocean reveal a diverse but patchy distribution of phycotoxins. *Toxicon*, **58**, 389–397.

Turner, A. D. and Goya, A. B. (2015) Occurrence and profiles of lipophilic toxins in shellfish harvested from Argentina. *Toxicon*, **102**, 32–42.

Twiner, M., Hess, P. and Doucette, G. J. (2014) Azaspiracids: toxicology, pharmacology, and risk assessment. In Botana, L. M. (ed.), *Seafood and Freshwater Toxins*. CRC Press, Boca Raton, USA, pp. 823–855.

Twiner, M. J., Rehmann, N., Hess, P. and Doucette, G. J. (2008) Azaspiracid shellfish poisoning: a review on the chemistry, ecology, and toxicology with emphasis on human health impacts. *Mar. Drugs*, **6**, 39–72.

Ueoka, R., Ito, A., Izumikawa, M., Maeda, S., Takagi, M., Shin-Ya, K., Yoshida, M., van Soest, R. W. M. *et al.* (2009) Isolation of azaspiracid-2 from a marine sponge *Echinoclathria* sp. as a potent cytotoxin. *Toxicon*, **53**, 680–684.

Vale, P., Biré, R. and Hess, P. (2008) Confirmation by LC–MS/MS of azaspiracids in shellfish from the Portuguese north-west coast. *Toxicon*, **51**, 1449–1456.

Yao, J., Tan, Z., Zhou, D., Guo, M., Xing, L. and Yang, S. (2010) Determination of azaspiracid-1 in shellfishes by liquid chromatography with tandem mass spectrometry. *Chin. J. Chromatogr.*, **28**, 363–367.

Yasumoto, T. and Takizawa, A. (1997) Fluorometric measurement of yessotoxins in shellfish by high-pressure liquid chromatography. *Biosci. Biotechnol. Biochem.*, **61**, 1775–1777.

Zharkikh, A. (1994) Estimation of evolutionary distances between nucleotide sequences. *J. Mol. Evol.*, **39**, 315–329.